J. Appl. Environ. Biol. Sci., 6(4S)43-54, 2016

ISSN: 2090-4274
Journal of Applied Environmental and Biological Sciences
www.textroad.com

A Thermosyphon driven Solar Water Heater Using CO_2 as Working Fluid

N. Abas[1,2], N. Khan[1],

[1]Department of Electrical Engineering, Comsats Institute of Information Technology, Park Road, Chak Shahzad, Islamabad.
[2]Department of Electrical Engineering, University of Gujrat, Hafiz Hayat Campus

Received: January7, 2016
Accepted: March 22, 2016

ABSTRACT

A density driven solar water heating system is designed, tested and reported here. This system comprises of an Evacuated Glass tube Solar Collector, a helical coil heat exchanger and a high pressure filling system. Carbon dioxide (R-744) is used as a mediating fluid in supercritical region. Solar heat raised R744 temperature from 35 to 78°C giving maximum temperature difference of 43°C. Temperature of R744 the at exit of the heat exchanger was measured to be 40°C at ambient temperature of 36°C. Heat exchanger raised the inlet water temperature from 26 to 55°C under off water tap condition in about 3 hours. In/out temperature difference of heated water was measured to be 27°C. We believe system efficiency can further increase if we use the system in mild sunshine, cold weather regions where system tends to operate around the critical point automatically with due to low heat input.

KEYWORDS: Heat exchanger, Shell & Helical Tube, Counterflow, Countercurrent

Nomenclature

A_c	Surface area of absorber tube (m^2)
C_p	Specific heat (J/kgK)
D	Diameter (m)
E	Specific enthalpy (kJ/kg)
F'	Collector efficiency factor
G	acceleration of gravity (m/s^2)
H	Heat transfer coefficient (W/m^2K)
I_T	Solar insolation (W/m^2)
K	Thermal conductivity (W/mK)
L	Helical coil tube length (m)
M	Mass flow rate (kg/s)
Nu	Nusselt number
P	Pressure (bar)
Pr	Prandtl number
Q	Energy gain (W/m^2)
Q_u	Useful heat gain (W)
Re	Reynolds number
S	surface are (m^2)
T	temperature (°C or K)
T_f	Mean temperature of CO_2 (°C)
T_a	Ambient temperature (°C)
Ra	Rayleigh number
U_L	Over-all loss coefficient (W/m^2K)

Subscripts

T	time (seconds or hrs)
m	mean or median
$\overline{T}$	Average temperature
i/o	internal/outer
w	width

Greek symbols

α	Dimensionless parameter
β	Dimensionless parameter
γ	Dimensionless parameter
χ	Correction factor
$\bar{\eta}$	Efficiency of collector
η_e	heat exchange efficiency
κ	ratio of ψ and M
ρ	density (kg/m^3)
Ψ	thermal constant per unit length (m^{-1})
θ	collector inclination angle
ξ	Boundary layer thickness (m)
λ_c	corrective factor
ϑ	Incidence angle
Φ	pressure drops ratio
υ	fluid velocity (m/s)

α	Dimensionless parameter
β	Dimensionless parameter
γ	Dimensionless parameter
χ	Correction factor
η_e	heat exchange efficiency
κ	ratio of ψ and M
ρ	density (kg/m^3)
Ψ	thermal constant per unit length (m^{-1})
θ	collector inclination angle
ξ	Boundary layer thickness (m)
λ_c	corrective factor
ϑ	Incidence angle
Φ	pressure drops ratio
υ	fluid velocity (m/s)

* **Corresponding Author:** N. Khan, Department of Electrical Engineering, University of Gujrat, Hafiz Hayat Campus
naeemk56@yahoo.com

1.0 INTRODUCTION

Carbon Dioxide (CO_2) is an environmental benign natural refrigerant initially used by Thaddon in 1886 in an early refrigeration system. CO_2 is abundantly available in the environment and as by product of many industrial applications. After the invention of synthetic refrigerants in 1930, it was replaced by Chlorofluorocarbons (CFC), Hydrocholoroflourocarbons (HCFC) and later by Hydrofluorocarbons (HFC) by virtue of their better thermal performance, safety and reliability[1,2]. CFC and HCFC were noted to cause depletion of the environment friendly ozone layer in 1985 and global communities posed abannedd on production and use of such refrigerant after 1995 underthe global treatyy named Montreal Protocol. CFC and HCFC were replaced with HFC which do not harm the ozone layer however, they significantly contribute to global warming. Kyoto Protocol (1997) allowed the use of HFC with time barred permission for the complete phasing out of HCFC by 2015-2020 and HFC by 2030. According to the Intergovernmental Panel on Climate Change (IPCC) the anthropogenic greenhouse gases are the major cause of augmented earth temperature, which is subsequently melting of glaciers raised ocean level [3]. Montreal Protocol (1997), F-gas (2015) law, Paris Agreement (2015) quest for low global warming refrigerants to uphold global average temperature well below 1.5 °C [4][5].

American Society of Heating and Refrigeration (ASHREA) envisaged [6] the use of natural refrigerants for next generation heating and cooling applications. Among these refrigerants Ammonia (NH_3) is toxic, water (H_2O) freezes in sub-zero, hydrocarbons (HC's) are flammable, and silicon oil is difficult to handle due to higher viscosity. CO_2 is non-toxic, non-freezing (-56.6 °C) non-flammable, having superior thermo physical properties in sub-zero temperature areas when used in density driven systems as described in our preceding work [7]. An evacuated glass tube solar collector (EGTSC) is designed, tested and reported here employing super critical CO_2 as a mediating fluid.

1. Thermodynamic Properties of CO_2 Fluid

Physical properties of the CO2 fluid (R-744) exhibit a radical change when temperatures and pressures are increased from normal to sub-critical, critical and supercritical points. CO_2 state variables such as internal energy, density, coefficient of compressibility, specific enthalpy and entropy go on increasing with increase in temperature and pressure from normal to sub-critical, critical and supercritical points. CO_2 specific heat capacity (Cp), Prandtl numbers (Pr), coefficient of thermal expansion (K), thermal diffusivity, viscosity (μ) and conductivity (k) exhibit nonlinear behavior in normal, sub-critical, critical and supercritical regimes. CO_2 fluid thermal diffusivity at critical point is 13.02 and 17.65 times lower compared to normal and supercritical regimes. Specific heat capacity (Cp) of R744 at critical point is 29.16 times higher compared to normal and 33.82 times higher compared to supercritical regimes. R744 specific heat plot for various temperatures and pressures at low increment step shows it may peak to 56kJ/kg at critical point. Specific heat capacity plot (cp) of R744 using Reference Fluid Thermodynamic and Transport Properties Database (REFPROP) [8] is shown in Fig. 1.

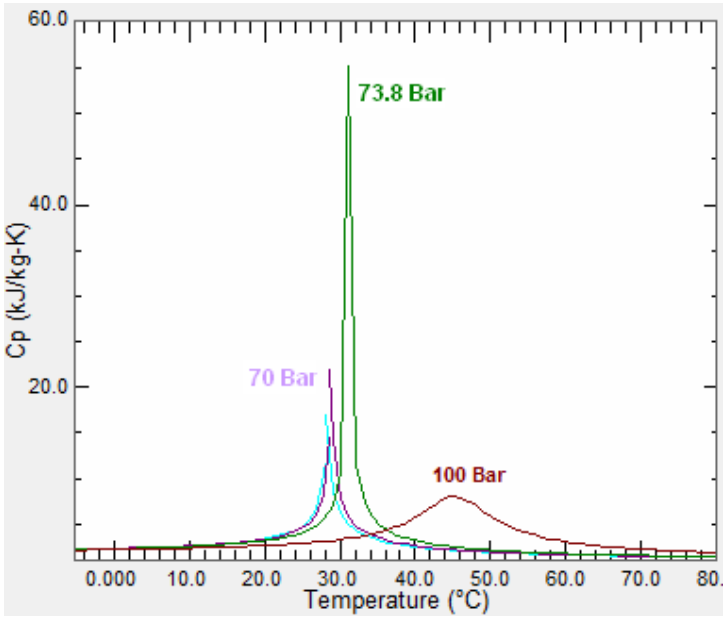

Fig.1 Variation of R744 specific heat (c_p) with temperature and pressure

R744 fluid thermal conductivity at critical point is 1.18 times lower than normal, but 1.16 times higher compared to sub-critical and 3.16 times higher than the supercritical regime. Prandtl number (Pr) defines fluid flow transition from laminar to turbulent regimes. R744 fluid Pr at critical point is 7.84 times larger than normal and 12.93 times larger compared to supercritical regimes. REFPRPO plot shows maximum value of R744 may peak to 15 at critical point. Prandtl number (Pr) plot for R744 using REFPRO is shown in Fig.2.

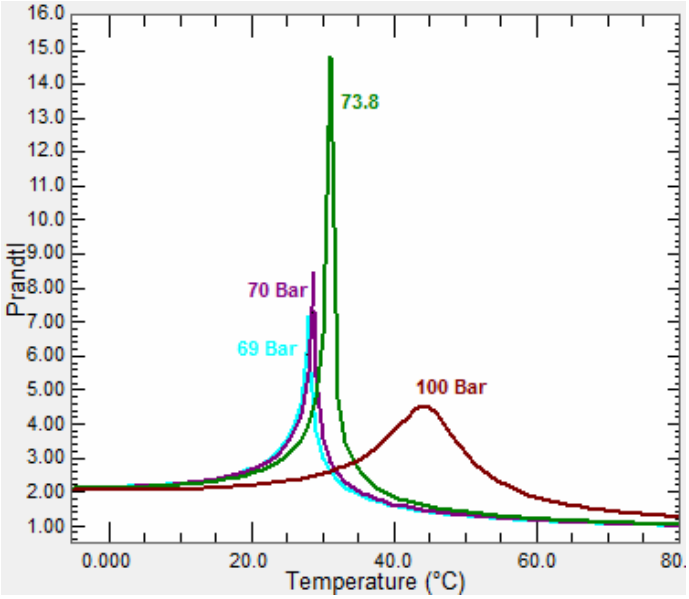

Fig.2 Variation of R744 Prandtl number with temperature and pressure.

Carbon dioxide fluid density (ρ) exhibits strange behavior at 28 to 29°C temperatures and 69 to 70 bar pressure. At sub-critical temperature (28°C) and pressure (69-bar) the density drops from about 670 to 380kJ/m^3 and at 28.5°C density declines from 640 to 300kJ/m^3. Density plot using REFPRO exhibits discontinuity from 28 to 29°C temperatures at 69 to 70-bar pressures. If pressure at 31.1°C is increased from 73.8-bar to 100 bar then the density of R744 increases from 369.7 to 760kJ/m^3. However, at critical temperature (31.1°C) and pressure (73.8-bar) the R744 exhibits almost free fall density drop from about 650 to 369.71kJ/m^3 as shown in Fig.3.

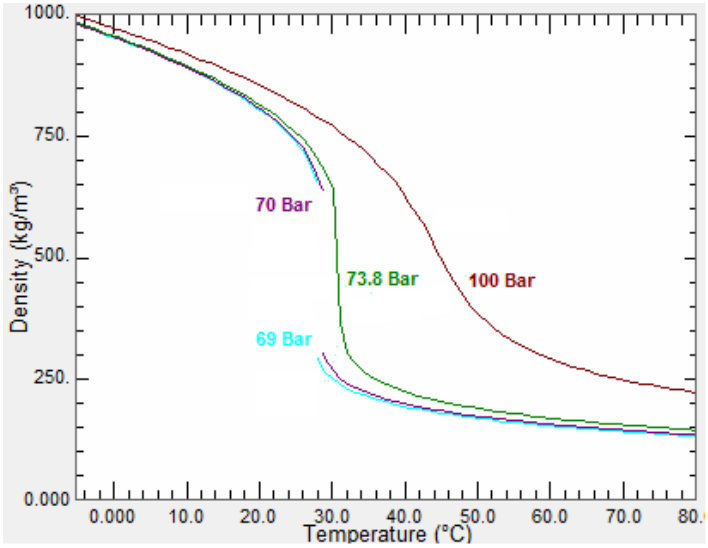

Fig.3 R744 density variation with temperature and pressure

Latest information about CO_2 refrigerant research worldwide is available from online resources [R744.com]. Physical properties of CO_2 in normal (T<-4°C and P<60 bar), sub-critical (T=20-28°C and P=60-71bar), critical (T=31.1°C and P=73.8 bar) and supercritical (T>31.1°C and P>74 bar) regimes may be calculated using the REFPRO are shown in Table 1.

Table 1: Thermodynamic state variables of carbon dioxide using REFPROP

Properties	Units	Normal	Sub-critical	Critical	Super critical
Pressure , P	bar	69	70	73.8	100
Temperature, T	C	-5	20	31.1	78
Heat capacity, c_P	kJ /kg K	2.218	3.305	64.67	1.913
Thermal conductivity	(mW /m.K	122.53	89.94	103.95	32.90
Prandtl-Number	--	2.119	2.648	16.55	1.282
Kinematic viscosity	cm^2/s	0.0012	0.0009	0.0007	0.0009
Thermal diffusivity	cm^2/s	0.0005	0.0003	0.00004	0.0007
Internal Energy	kJ/kg	178.80	241.29	339.42	422.85
Enthalpy	kJ/kg	185.83	249.95	359.38	467.08
Density,ρ	kg/m^3	981.61	808.60	369.71	226.08

A triple point is the joining point of solid, liquid and gas phase, whereas the supercritical point is joining point of liquid, gas and supercritical fluid boundaries. Temperature and pressure associated with critical point are much higher than those of triple point. Triple and critical points associated with solid, liquid, gas and supercritical fluid phases of carbon dioxide (R744) are shown in Fig.4 [9][10–13].

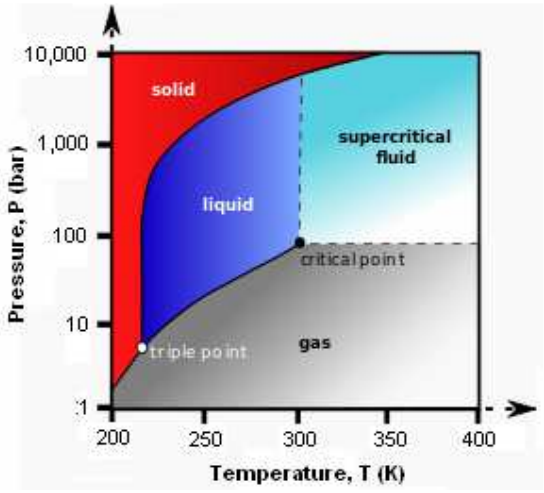

Fig.4 R744 triple and critical points [9]

Carbon dioxide large heat carrying capacity at supercritical point causes density, specific heat, viscosity, thermal conductivity and Prandtl numbers variations which allow natural convection to circulate fluid in close loop. If temperature and pressure are locked to the critical point, where heat capacity and density are many times higher than normal, the coefficient of performance (COP) increases significantly even if we use fluid circulation pump.

2. Steady State Heat Transfer

Heat exchangers efficiently transfer thermal energy from heating (hot) to heated (cold) fluids. Heating and heated fluids carrying metal tubes are thermally connected to avoid physical mixing of fluids. Natural countercurrent flow heat exchange biological processes include human breathing (nasal passages), animal carotid rete in hoofed animals and blood circulation in wading birds and fish. Heat exchange industrial processes include space heating, engine oil-fuel flow, refrigeration and air conditioning. Any heat exchanger may take counter flow (countercurrent) or parallel flow (concurrent) horizontal or vertical configurations. High pressure heat exchangers such as supercritical CO_2 working over 80-bar usually takes the form of a shell and tube coil. Coil folds, baffle, tube pitch and diameter size depend on heating demand. The thin tube design remains efficient and economic but fouls up fast. Space constraint designs may go for self cleaning Spiral Heat Exchangers (SHE) in pursuance of techno-economic tradeoffs. Heating and heated fluids flow in opposite directions in countercurrent flow heat exchangers.

A heat exchanger may consist of hot and cold fluids carrying tubes thermally connected with each other. In steady state the temperature profiles are not functions of time. Newton's cooling law may be used to write two heat transfer equations between two thermally connected (Ψ) fluids [14]

$$du_P/dt = \Psi(T_S - T_P) \quad (1)$$

$$du_S/dt = \Psi(T_P - T_S) \quad (2)$$

Assuming heating and heated fluids have mass flow rates of m_P and m_S with mean heat capacities of C_{ppm} and C_{psm} respectively. The time rate of change for the fluid element being carried along by the flow is

$$du_P/dt = M_P\, dT_P/dx \quad (3)$$

$$du_S/dt = M_S\, dT_S/dx \quad (4)$$

Here thermal mass flow rate $M_i = C_{ipm}.m_i$ wherein subscript i refers to p (hot) and s (cold) fluids. Comparing (1) and (2) with (3) and (4) the coupled differential equations governing heat transfer become

$$dT_P/dx = \kappa_P(T_S - T_P) \quad (5)$$

$$dT_S/dx = \kappa_S(T_P - T_S) \quad (6)$$

Where $\kappa_p = \Psi/M_P$, $\kappa_S = \Psi/M_S$ and $\kappa = \kappa_P + \kappa_S$. Solution of the first order coupled differential equations (5) and (6) yields

$$T_P = C' - \frac{C''\kappa_P}{\kappa} e^{-\kappa x} \quad (7)$$

$$T_S = C' + \frac{C''\kappa_S}{\kappa} e^{-\kappa x} \quad (8)$$

Where C' and C'' are integration constants.

If T_{P1} & T_{P2} and T_{S1} & T_{S2} are temperatures at entrances and exits of heating and heated fluids tubes of length L then under steady-state conditions the average temperatures in heating ($\overline{T}_P$) and heated ($\overline{T}_S$) fluids are

$$\overline{T}_P = \frac{1}{L}\int_0^L T_P(x)dx \quad (9)$$

$$\overline{T}_S = \frac{1}{L}\int_0^L T_S(x)dx \quad (10)$$

Temperatures at the entrance and exit ports of heating fluid tube are

$$T_{P1} = C' - C''\kappa_P/\kappa \quad (11)$$

$$T_{P2} = C' - \frac{C''\kappa_P}{\kappa} e^{-\kappa L} \quad (12)$$

From (9), (11) and (12) the average temperature in heating fluid is

$$\overline{T}_P = C' - \frac{C''\kappa_P}{\kappa^2 L}(1 - e^{-\kappa L}) \quad (13)$$

Similarly temperatures at the entrance and exit of the heated fluid tube are

$$T_{S1} = C' + C''\kappa_S/\kappa \quad (14)$$

$$T_{S2} = C' + \frac{C''\kappa_S}{\kappa} e^{-\kappa L} \quad (15)$$

From (10), (14) and (15) the average temperature in heating fluid is

$$\overline{T}_S = C' + \frac{C''\kappa_S}{\kappa^2 L}(1 - e^{-\kappa L}) \quad (16)$$

Experimentally, it is possible to find the entrance and exit temperatures of heating as well as heated fluid tubes using temperature gauges. Choice of any two temperatures can allow elimination of integration constants. A typical plot of temperatures in counter flow heat exchanger is shown in Fig.5.

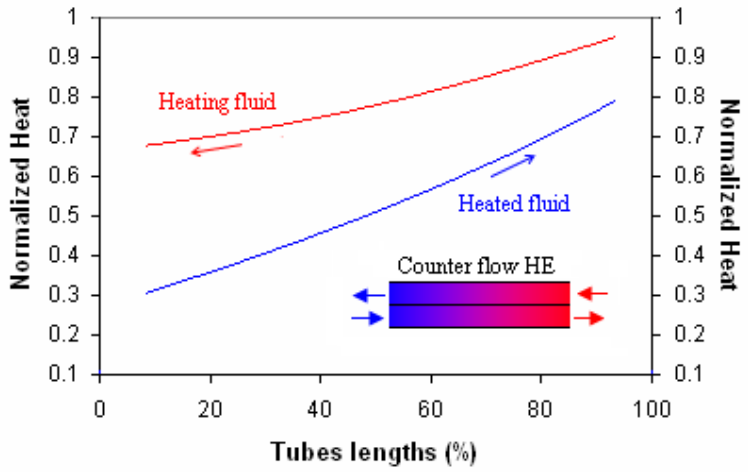

Fig.5 Coupled heat transfer in a counter flow heat exchanger.

Overall heat transfer rates between fluids carrying tubes are

$$\frac{dU_P}{dt} = \int_0^L \frac{dU_P}{dt} dx = M_P(T_{P2} - T_{P1}) = \Psi L(\overline{T}_S - \overline{T}_P) \tag{17}$$

$$\frac{dU_S}{dt} = \int_0^L \frac{dU_S}{dt} dx = M_S(T_{S2} - T_{S1}) = \Psi L(\overline{T}_P - \overline{T}_S) \tag{18}$$

The quantity $(\overline{T}_P - \overline{T}_S)$ is known as mean log temperature difference. LMTD is a measure of effectiveness of the heat exchanger in transferring heat energy from heating to heated fluid.

$$Q = U \times S \times LMTD \tag{19}$$

Heat exchanged at any location z may be

$$q = \frac{U}{D}\left[T_S(z) - T_P(z)\right] \tag{20}$$

According to Fourier's law

$$dT_P/dz = k_P\left(T_P(z) - T_S(z)\right) = -k_P \Delta T(z) \tag{21}$$

$$dT_S/dz = k_S\left(T_S(z) - T_P(z)\right) = -k_S \Delta T(z) \tag{22}$$

Where $k = k_P + k_S$. Subtraction of (22) from (21) gives

$$\frac{d\Delta T}{dz} = \frac{d(T_S - T_P)}{dz} = \frac{dT_S}{dz} - \frac{dT_P}{dz} = k\Delta T(z) \tag{23}$$

Heat exchanged along tube length may be given by

$$Q = \int_P^S q(z)dz = \frac{U}{D}\int_P^S \Delta T(z)dz = \frac{U}{D}\int_P^S \Delta T dz \tag{24}$$

$$Q = \frac{US}{(S-P)}\int_P^S \Delta T dz = US\left(\int_P^S \Delta T dz \Big/ \int_P^S dz\right) \tag{25}$$

$$Q = US\int_{\Delta T(P)}^{\Delta T(S)} \Delta T \frac{dz}{d\Delta T} d(\Delta T) \Big/ \int_{\Delta T(P)}^{\Delta T(S)} \Delta T \frac{dz}{d\Delta T} d(\Delta T) = US\int_{\Delta T(P)}^{\Delta T(S)} \Delta T \frac{1}{k} d(\Delta T) \Big/ \int_{\Delta T(P)}^{\Delta T(S)} \Delta T \frac{1}{k\Delta T} d(\Delta T) \tag{26}$$

$$Q = US\left(\Delta T_I - \Delta T_{II}\right) / \ln\frac{\Delta T_I}{\Delta T_{II}} \tag{27}$$

Comparing (19) to (27) and taking ΔT_I =GTD and ΔT_{II} =LTD the LMTD is

$$\text{MLTD} = (GTD - LTD)/\ln\left(\frac{GTD}{LTD}\right) \quad (28)$$

Where GTD or $\Delta T_I = T_{P1}-T_{S2}$ and LTD or $\Delta T_{II} = T_{P2} - T_{S1}$. This method is limited to counter flow heat exchanger as it can not be applied to the multiple pass shell and tube type heat exchangers in which MLTD needs a correction factor χ as follows

$$\text{MLTD} = F \times \underline{MLTD} \quad (29)$$

Parameter F is given by

$$F = \left(1 - \left((RP-1)/(P-1)\right)^{1/N}\right)/\left(R - \left((RP-1)/(P-1)\right)^{1/N}\right) \quad (31)$$

Two variable R and P are given by

$$R = (T_{P1} - T_{P2})/(T_{S2} - T_{S1}) \quad (30)$$

$$P = (T_{S2} - T_{S1})/(T_{P1} - T_{S1}) \quad (32)$$

Where N is the number of passes (turns) of the hot fluid tube through the shell-and-coil counter flow heat exchangers. Values of correction factors may directly be obtained using R and P from the published charts in standard text books [15]. Counterflow heat exchangers are more efficient than parallel flow heat exchangers. Parallel flow heat exchangers are used for liquid and solid phase fluids and counter flow type for the gas-gas and gas-liquid fluids. The mass flow rate of CO_2 under thermosyphon driven system is very low in the range of 0.01 to 0.8 kg/s but specific heat increases thousands times at supercritical point. Counter flow heat exchanger must be vertical for gas phase fluids, especially, the CO_2 vapors heating water using thermosiphon principle.

3. Physical Model and governing equations

Instantaneous heat balance on collector may be expressed by [16]

$$\dot{Q} + M_P \frac{dT_P}{dt} = A\eta_{ce}\vartheta I - Ah(T_P - T_a) \quad (33)$$

Where ϑ is incidence angle modifier, η_{ce} is collector efficiency, A collector surface area and I is solar irradiance (W/m^2). Instantaneous heat balance for the coil surface area S in heat exchanger becomes

$$M_S \frac{dT_S}{dt} = \dot{Q} - US(T_S - T_a) \quad (34)$$

Overall heat transfer may be given by

$$\dot{Q} = US(T_P - T_a) \quad (35)$$

If $dT_c/dt = dT_{xr}/dt$ then from (33), (34) and (35)

$$\dot{Q}\left(1 + \frac{M_P}{M_S}\right) = A\eta_{ce}\vartheta I + \frac{M_P}{M_S}US(T_S - T_a) - Ah(T_P - T_a) \quad (36)$$

For M_P/M_S =0.04 (36) may be rewritten for instantaneous heat balance as

$$\dot{Q} = A\eta_{ce}\vartheta I - Ah(T_P - T_a)/\left(1 + \frac{M_P}{M_S}\right) \quad (37)$$ From (35) and (37) we can obtain

$$\dot{Q} = C_1\vartheta I - C_2(T_S - T_a) \quad (38)$$

Where C_1 and C_2 are constants

Or alternatively for the evacuated glass tube solar collector employing U-shape heat collection tube the amount of collected heat can be calculated as[17]

$$Q_u = F' A_c\left[I_T(\alpha\bar{\tau}) - U_L(T_f - T_a)\right]; \quad \eta = \frac{Q_u}{I_T A_c} \quad (39)$$

4. Thermosiphon Force

Evolution of natural thermosiphon force under varying temperature dependent density change is a wonderful phenomenon. We know objects feel weighing less in liquids than in the air due to buoyancy. Any object of thickness h and area A at depth s

underwater experiences a downward force of ρgsA due to its own weight and an upward force of ρg(h+s)A due to buoyancy. Resultant buoyant force F_B is given by

$$F_B = \rho g(h+s)A - \rho gsA = \rho ghA = \rho gV \quad (39)$$

The buoyant force on a body immersed in a fluid is equal to the weight of the fluid displaced by body acting upward against the gravity. A liquid or gas in a vertically erected cylindrical column under temperature change starts flowing upward against gravity under the thermosiphon effect. Hotter gas or liquid molecules become lighter than colder molecules of the bulk medium. Variation of fluid density with temperature may be better understood by its volume expansion coefficient β given by

$$\beta = \frac{1}{\nu}\left(\frac{\partial \nu}{\partial T}\right)_P = \frac{1}{\rho}\left(\frac{\partial \rho}{\partial T}\right)_P \quad (40)$$

The change in density Δρ may be given in terms of change in temperature ΔT by

$$\Delta\rho = \rho\beta\Delta T \quad (41)$$

We know the volume expansion coefficient β = 1/T, therefore

$$\Delta\rho = \rho\Delta T/T \quad (42)$$

Role of Reynolds numbers in forced convection is played by Grashof numbers in natural convection. Grashof number for fluid flow under natural convection is given by

$$Gr = \frac{g\Delta\rho V}{\rho\nu^2} = \frac{g\beta\Delta T V}{\nu^2} = \frac{g\beta(T_{surf} - T_{Bulk})\delta^3}{\nu^2} \quad (43)$$

Where δ is characteristic length, ν is kinematic viscosity, T_{surf} surface and T_{bulk} bulk fluid temperatures. In case of CO_2 fluid the variation of density at critical temperature is many folds of normal density that creates a natural circulation force. Average Nusselt number in natural convection in terms of Prandtl number (Pr) is given by

$$Nu = \frac{h\delta}{k} = C(Gr\,\mathrm{Pr})^n = C(Ra)^n = \frac{g\beta(T_{surf} - T_{Bulk})\delta^3}{\nu^2}\mathrm{Pr} \quad (44)$$

Where Ra is the Rayleigh number. The value of n is ¼ for laminar flow and 1/3 for turbulent flows. The value of C is usually less than 1.

To calculate gravity driven thermosiphon buoyancy pressure, we follow Koffi's method [18][19]. The buoyant pressure produced by solar collector in thermosiphon loop is given by [20]

$$P_{BP} = g\rho\phi\sin\theta\int_0^{L_C}(T(x) - T)dx \quad (45)$$

where T(x) is temperature at location x in collector. According to Close [21]

$$T(x) - T_i = x(T_{f2} - T_{f1})/L_c \quad (46)$$

From equations (45) and (46) we can obtain

$$P_{BP} = \frac{g\rho\phi\sin\theta}{L_c}\int_0^{L_c}\frac{T_{f2} - T_{f1}}{L_c}xdx \quad (47)$$

Integration of (47) gives

$$P_{BP} = g\rho\phi\sin\theta\frac{L_c}{2}(T_{f2} - T_{f1}) \quad (48)$$

Total pressure drop in thermosiphon loop is equal to sum of pressure drops in the collector, connection tubes and heat exchanger.

$$\Delta P_L = \Delta P_c + \Delta P_t + \Delta P_{he} \quad (49)$$

Pressure drops in the solar collector, tubes and heat exchanger for fluid speed of υ $(= 4\dot{m}/\rho\pi d^2)$ are given by [22]

$$\Delta P_c = 128\upsilon L_c\dot{m}/\pi N_c d_c^4 \quad (50)$$

$$\Delta P_t = 32\rho\upsilon_t L_t\upsilon/d_t^2 \quad (51)$$

$$\Delta P_{he} = 8k\dot{m}/\rho\pi^2 d_{he}^4 \quad (52)$$

For $\Phi = \Delta P_c/\Delta P_t$ total pressure drop may be given by

$$\Delta P_L = 8k\dot{m}/\rho\pi^2 d_{he}^4 + (1+\Phi)128\upsilon L_c\dot{m}/\pi N_c d_c^4 \quad (53)$$

Heat and mass transfer balance equation in terms of thermosiphon buoyancy pressure and pressure losses in all sections of the loop may be written as

$$P_{BP} = g\rho\phi \sin\theta \frac{L_c}{2}(T_{f2} - T_{f1}) = 8k\dot{m}/\rho\pi^2 d_{he}^4 + (1+\Phi)128\upsilon L_c \dot{m}/\pi N_c d_c^4 \qquad (54)$$

This equation can give the value of instant pressures in thermosiphon loop. Usually the pressure drop across loop is about 100psi in CO_2 refrigerant solar water heaters. It allows the calculation of heating fluid flow rate. Above equation considers pressure drop loss in connection tubes between solar collector and heat exchanger. If we consider pressure drops in the solar collector and heat exchanger then [23] thermal mass flow capacity may be given by

$$M_P = \sqrt{\frac{gN\pi Ad^4(0.5L\sin\theta + H)}{128L(1+\vartheta)}} \sqrt{\left(\frac{\rho_o \beta}{\nu c_P} F'[I(\tau\alpha) - U(T_m - T_{amb})\right)} \qquad (55)$$

Where F′ depends on the geometry. It allows the calculation of thermosiphon flow rate.

4. Experimental Setup

A solar collector consisting of nine 58×47×1800mm size borosilicate evaluated glass tubes (China make) is altered to work for Carbon dioxide as mediating fluid. Glass tubes were placed inclined in aluminum stand facing south at a local latitude angle of Islamabad, Pakistan (33° 44' 16.9620" N). Copper tubes were bent with stainless steel (Parker makes) benders of 1/4″ and 3/8 ″ sizes. These tubes were wrapped in aluminum foil to act as a fin between glass and copper tube. Copper tubes were sealed from top using wooden corks. The heat was collected by high pressure endurance capacity copper tubes with 6.35mm external and 4.6mm internal diameters. The connection copper tubes and headers between solar collector and the heat exchangers were covered by insulating urethane materials. Helical coil in heat exchanger was fabricated out of high pressure enduring copper tubes with 9.25mm external and 7.75mm internal diameters. Copper u-tubes were connected to upper and lower stainless steel 800.89×21.5×15.5 mm (schedule 40) Parker headers. Copper U-tubes transfer heat from evacuated glass tubes into upper header connected to the upper input port of heat exchanger. Cold CO_2 refrigerant, after transferring heat, returns back into lower stainless steel header to repeat the cycle. The copper tubes were connected to the headers by stainless steel (1/4 ″ NTP, 6000psi) Parker couplers using argon welding. We used ¼ ″ NTP Parker make needle valves, 3-way ball valves and non return valve. SS connector unions, sockets, dead plugs, connectors, couplers, male elbow, male connector and female branch Tee (3/8 ″) were used to fabricate the collector. Carbon dioxide gas filling system consists of 3/8 ″ Parker make (6000psi) pipe and stainless steel (1/4 ″ FNTP) three way filling valve. Temperature and pressure measurements were monitored by 0-400°C analog temperature (Italy make) and 0-400bar pressure (Wiki Germany make) gauges. Heat exchanger was fabricated in local market using available insulation and construction materials. The design and inclination copper U tubes and headers are discussed in details in our earlier work.[24,25] of First trial led to puncture of high pressure tube which was amended using soldering inthe second phasee. Picture of completed experimental set with isometric view up is shown in Fig.6.

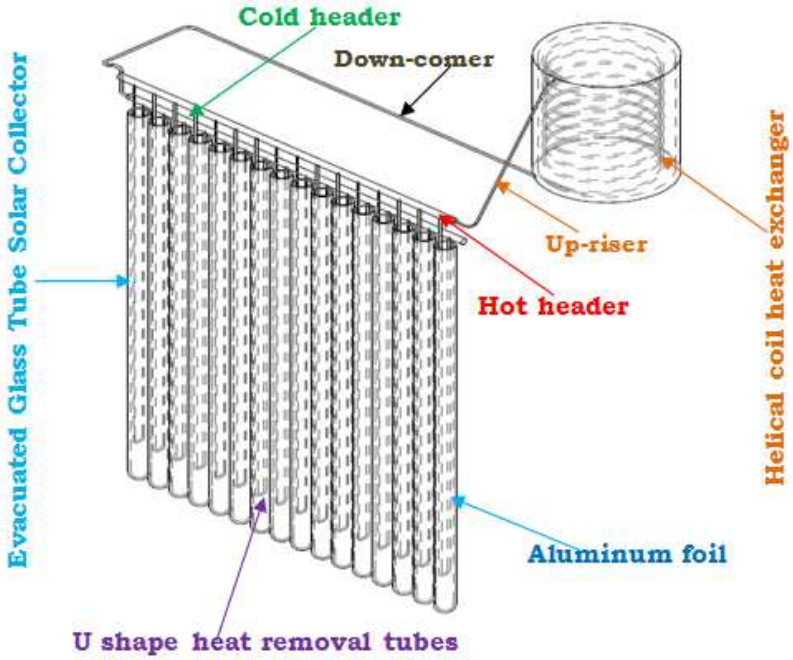

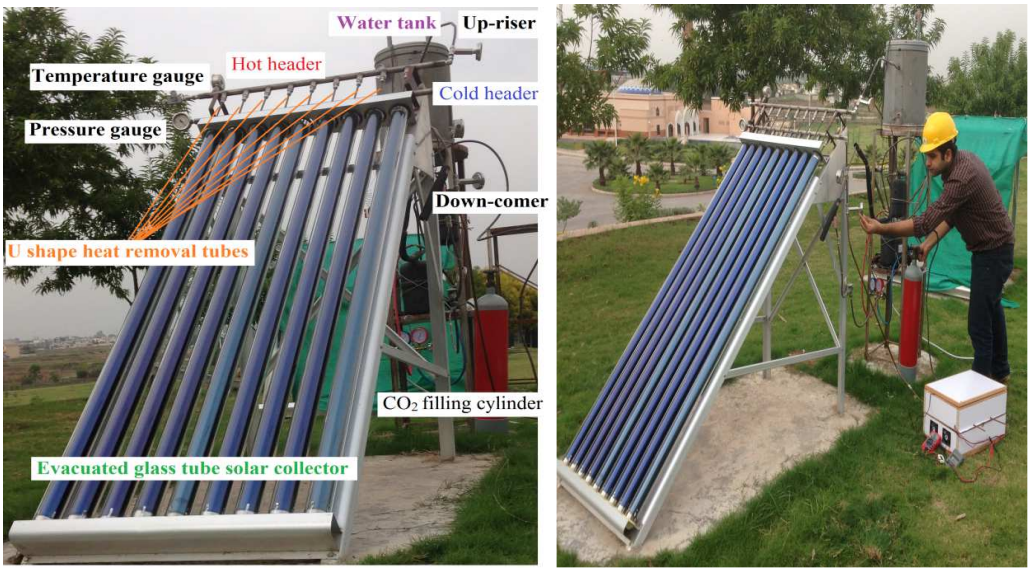

Fig.6 Experimental layout of solar water heater using R744 refrigerant.

Parameters of solar collector using R744 as working fluid are shown in Table 2.

Table 2: Solar collector aperture area of glass tubes

Evacuated glass tube length L (m)	=	1.8		Tube outer diameter (m)	
=	0.00058	Tube inner diameter (m)	=	0.00047	
Evacuated glass surface area (m^2)	=	0.0016390			
Total no. of glass tubes	=	09	Tubes collector surface area (m^2)	=	1.475172

Solar collector aperture area was calculated using $A = \pi \times r \times L$. Engineering parameters of heat exchanger are shown in Table 3.

Table 3: Heat exchanger helical copper tube parameters

Tube size (m)	=	0.009525	Tube wall thickness (m)	=	0.00075
Tube size (m)	=	0.008025	Tube length (m)	=	5.334
Tube outer surface area (m^2)	=	0.15953			

Copper tubes surface area was calculated using $A = \pi \times D \times L$

Complete experimental system was placed under sun on November 15, 2015. Solar water heater using R744 as working fluid exhibited following temperatures after three hours exposure to sunlight.

CO_2 temperature (T_{P1})	at entrance of heat exchanger	=	78°C
CO_2 temperature (T_{P2})	at exit of heat exchanger (HE)	=	40°C
Water tank initial temperature (T_{S1})	at entrance of HE	=	26°C
Water tank initial temperature (T_{S2})	at exit of HE	=	55°C
Ambient air temperature on October 1, 2012 at 3PM		=	37°C

GTD	=	$T_{P1} - T_{S2}$	78-55	=	23
LTD	=	$T_{P2} - T_{S1}$	40 – 26	=	14

$$LMTD = \frac{GTD - LTD}{\ln(GTD / LTD)} = \frac{23 - 14}{\ln(23/14)} = \frac{9}{0.4964} = 18.13$$

If GTD and LTD values are reversed then

GTD = ΔT_L = $(T_{P2} - T_{S1})$ = (40 – 26) = 14°C

LTD = ΔT_o = $(T_{P1} - T_{S2})$ = (78 – 55) = 23°C

$$LMTD = \frac{GTD - LTD}{\ln(GTD / LTD)} = \frac{14 - 23}{\ln(14/23)} = \frac{-9}{-0.49659} = 18.12$$

It means if GTD and LTD values are even reversed by human error or by reverse thermosiphon effect it does not appreciably affect value of LMTD.

5. Conclusions

A thermosiphon solar water heater using carbon dioxide as working fluid was designed, fabricated, and operated successfully. During testing and operation, it was noted reverse siphoning starts if supposed hot and cold headers are placed at the same heights. Hot header has to be higher than cold header to block reverse thermo siphoning. If higher and lower level does not stop reverse thermo siphoning then copper pipe from upper header to heat exchanger may be given few centimeter extra top down bending. Carbon dioxide was filled at 68bar which approached the critical point (73.38bar and 31.1 (C) within few minutes of sun exposure. No attempt was made to control the temperature and pressure, therefore, as thermosiphon effect proceeded in the supercritical regime at 78°C temperature and 76-bar pressure within three hours. If temperature and pressure are controlled around critical point then coefficient of performance may increase due to exponential increase in specific heat at constant pressure.

Acknowledgements

This research was in part, supported by a grant from the Pakistan-US Science and Technology Cooperation Program (Project ID No. 299), US Department of State (jointly administered by the National Academics and Higher Education Commission of Pakistan).

REFERENCES

[1] Nations U. KYOTO PROTOCOL TO THE UNITED NATIONS FRAMEWORK CONVENTION ON CLIMATE CHANGE. 1987.

[2] Nations U. The Montreal Protocol on Substances that Deplete the Ozone Layer. 1997.

[3] IPCC. A report of Working Group I of the Intergovernmental Panel on Climate Change. 2007.

[4] Commission E. Paris Agreement. 2015.

[5] Abas N, Kalair A, Khan N. Review of fossil fuels and future energy technologies. Futures 2015;69:31–49. doi:10.1016/j.futures.2015.03.003.

[6] ASHREA. ASHREA position document on Natural Refrigerants. 2011.

[7] Abas N, Khan N. Carbon conundrum, climate change, CO2 capture and consumptions. J CO2 Util 2014;8:39–48. doi:10.1016/j.jcou.2014.06.005.

[8] Lemmon EW, Huber ML, Mclinden MO. REFPRO, NIST Reference Fluid Thermodynamic and Transport Properties Database (REFPROP): Version 9.1 2012.

[9] Jacobs, M.A. Measurement and modeling of thermodynamic properties for the processing of polymers in supercritical fluids. Eindhoven University of Technology, 2005.

[10] Span R, Wagner W. A New Equation of State for Carbon Dioxide Covering the Fluid Region from the Triple-Point Temperature to 1100 K at Pressures up to 800 MPa. J Phys Chem Ref Data 1996;25:1509–96.

[11] Fenghour, A., Wakeham, W.A., Vesovic V. The Viscosity of Carbon Dioxide. J Phys Chem Ref Data 1998;27:31–44.

[12] Vesovic, V., Wakeham, W.A., Olchowy, G.A., Sengers, J.V., Watson JTR, and Millat J. The transport properties of carbon dioxide. J Phys Chem Ref Data 1990;19:763–808.

[13] Rathjen, W. and Straub J. Temperature dependence of surface tension, coexistence curve, and vapor pressure of CO2, CClF3, CBrF3, and SF6. Heat Transf. Boil., New York: Academic Press; 1977.

[14] Kay JM (John M, Nedderman, M R. Fluid mechanics and transfer processes. New York: Cambridge University Press; 1985.

[15] Ghoshdastidar PS. Heat Transfer. Oxford Higher Education/Oxford University Press; 2012.

[16] Annaratone D. Handbook for Heat Exchangers and Tube Banks Design. Springer; 2010.

[17] Ma L, Lu Z, Zhang J, Liang R. Thermal performance analysis of the glass evacuated tube solar collector with U-tube. Build Environ 2010;45:1959–67. doi:10.1016/j.buildenv.2010.01.015.

[18] Koffi PME, Andoh HY, Gbaha P, Touré S, Ado G. Theoretical and experimental study of solar water heater with internal exchanger using thermosiphon system. Energy Convers Manag 2008;49:2279–90. doi:10.1016/j.enconman.2008.01.032.

[19] Kalogirou SA, Papamarcou C. Modelling of a thermosyphon solar water heating system and simple model validation. Renew Energy 2000;21:471–93. doi:10.1016/S0960-1481(00)00086-0.

[20] Duffie JA, Beckman WA. Solar Engineering of Thermal Processes. 4th ed. New Jersy: John Wiley & Sons Inc; 2006.

[21] Close DJ. A design approach for solar processes. Sol Energy 1967;11:112–22. doi:10.1016/0038-092X(67)90051-5.

[22] Joulie R. Applied Fluid Mechanics. Paris: Ellipses; 1998.

[23] Zerrouki A, Boumédien A, Bouhadef K. The natural circulation solar water heater model with linear temperature distribution. Renew Energy 2002;26:549–59. doi:10.1016/S0960-1481(01)00146-X.

[24] Abas N, Khan N, Hussain I. A Solar Water Heater for Subzero Temperature Areas. Prog. Sustain. Energy Technol. Gener. Renew. Energy, Cham: Springer International Publishing; 2014, p. 369–77. doi:10.1007/978-3-319-07896-0_20.

[25] Abas N, Nawaz R, Khan N. Parametric Quantification of Low GWP Refrigerant for Thermosyphon Driven Solar Water Heating System. Procedia Comput Sci 2015;52:804–11. doi:10.1016/j.procs.2015.05.136.